Towards NLO corrections to massive $gg \to VV$ production for off-shell Higgs studies at the LHC

Olivier Witteveen
Supervisor: Raoul Röntsch

I Abstract

We consider the production of two on-shell massive vector bosons through the "prompt" production process $gg \to VV$ and the production mediated by the exchange of a Higgs boson $gg \to H \to VV$. We present an interpolation method that allows the Monte Carlo (MC) integration of the two-loop massive amplitudes for $gg \to VV$ to be performed with only $\sim 10^3$ points evaluated in the phase space, while maintaining sufficient numerical control for phenomenological studies at the Large Hadron Collider (LHC). A standard MC implementation, requiring $\sim 10^4$ points to be evaluated in the phase space, would not be practical due to the computational intensity required to obtain the two-loop amplitudes. The method is tested at leading-order (LO) in a variety of cases, and compared against results at LO obtained using an automatic one-loop provider. Limitations of the method are discussed.

II Introduction

The Higgs mechanism, a central aspect of the Standard Model (SM), is a theoretically consistent description of the origin of elementary particle masses. The Higgs boson, which was found during Run I at the Large Hadron Collider (LHC) [1, 2], is a physical manifestation of this mechanism. An important task for Run II and beyond at the LHC is a thorough experimental study of the properties of the Higgs. The subsequent comparison against the properties predicted from theory provides a critical step in the verification of the SM. Any deviation found would be an indication that the electroweak symmetry-breaking mechanism, as currently described by the SM, is incomplete. A comprehensive exploration of the Higgs sector is therefore essential for both understanding the SM and for probing potential New Physics effects.

The majority of Higgs bosons studied at the LHC are on-shell, as this is where the majority of events lie. Despite this, the off-shell region in gluon fusion is well-populated − this was first realised by Kauer and Passarino [3]. For $gg\,(\to H) \to VV$, with $V = W$ or Z, about 10% of events come from the region $m_{VV} > 2m_V$. Studying off-shell Higgs production can give powerful insights into its properties. For instance, it was proposed by Caola and Melnikov [4] that the ratios of on- and off-shell cross sections can be used to indirectly constrain the Higgs width. The upper bounds obtained through this method ($\Gamma_H \sim \mathcal{O}(10\text{ MeV})$) are far more stringent than direct constraints on the Higgs width ($\Gamma_H < 1\,\text{GeV}$) which are limited by detector resolution [5–10]. The proposal assumes that on- and off-shell couplings of the Higgs boson to SM particles are identical. Even if this assumption is not true, analysing off-shell Higgs events may still provide vital insights into the nature of the Higgs couplings.

We are considering Higgs production through gluon-gluon fusion and subsequent decay into two on-shell vector bosons, $gg \to H \to VV$. However, the signal amplitude $gg \to H \to VV$ has identical initial and final states as the "prompt" production amplitude $gg \to VV$, and hence interference occurs between the two processes. As is well known, the interference is large and destructive at regions of high invariant mass, due to the fact that the Higgs mechanism in the SM is responsible for unitarising massive scattering amplitudes (see e.g. [3]). That brings us to another reason to study off-shell Higgs production: we can probe this unitarising mechanism using off-shell events.

We now discuss the current status of theoretical predictions for off-shell Higgs production. In order to do so, it is useful to split up the total transition amplitude $\mathcal{A}_{\text{tot}}$ for $gg\,(\to H) \to VV$ into contributions from the Higgs-mediated amplitude and the background amplitude. This yields:

$$|\mathcal{A}_{\text{tot}}|^2 = |\mathcal{A}_{\text{sgn}} + \mathcal{A}_{\text{bkgd}}|^2 = |\mathcal{A}_{\text{sgn}}|^2 + |\mathcal{A}_{\text{bkgd}}|^2 + 2\text{Re}\left[\mathcal{A}^*_{\text{sgn}}\mathcal{A}_{\text{bkgd}}\right]. \tag{1}$$

We can then separate the background amplitudes into contributions that include massive top quarks in the loop and those that do not[1]:

$$\mathcal{A}_{\text{bkgd}} = \mathcal{A}_{\text{bkgd,0}} + \mathcal{A}_{\text{bkgd,m}}, \tag{2}$$

and further into one-loop and two-loop contributions, denoted with $^{(1)}$ and $^{(2)}$ respectively:

$$\mathcal{A}_{\text{bkgd}} = \mathcal{A}^{(1)}_{\text{bkgd,0}} + \mathcal{A}^{(2)}_{\text{bkgd,0}} + ... + \mathcal{A}^{(1)}_{\text{bkgd,m}} + \mathcal{A}^{(2)}_{\text{bkgd,m}} + ... \tag{3}$$

where the ellipsis is used as a placeholder for higher order terms, beyond next-to-leading-order (NLO). The one-loop amplitudes are the leading-order (LO) contributions, whereas the two-loop amplitudes constitute the virtual NLO corrections.

We can do the same for the signal amplitude. In this case, to very good approximation, only the contributions from top quark loops need to be considered:

$$\mathcal{A}_{\text{sgn}} = \mathcal{A}^{(1)}_{\text{sgn}} + \mathcal{A}^{(2)}_{\text{sgn}} + ... \tag{4}$$

Representative Feynman diagrams for the one-loop (LO) amplitudes of both the signal and background process are shown in figures 1a and 1b respectively. Similarly, figure 2 shows a representative Feynman diagram for the two-loop amplitudes of $gg \to VV$ prompt production.

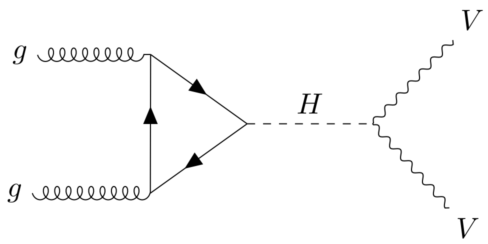

(a)

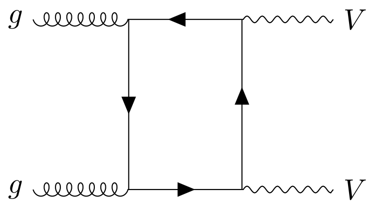

(b)

Figure 1: Representative Feynman diagrams for (a) the signal amplitude ($gg \to H \to VV$) and (b) the background amplitude ($gg \to VV$) at LO.

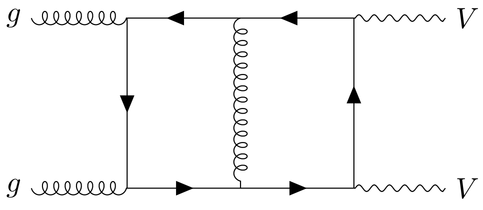

Figure 2: Representative Feynman diagram for two-loop corrections to the prompt production background amplitude ($gg \to VV$).

[1]In the case of WW production, contributions with top quarks in the loop also include bottom quarks, which can be treated as either massive or massless.

Taking the modulus squared of equation 3 yields:

$$\begin{aligned}|\mathcal{A}_{\text{bkgd}}|^2 = &\underbrace{|\mathcal{A}^{(1)}_{\text{bkgd,0}}|^2 + |\mathcal{A}^{(1)}_{\text{bkgd,m}}|^2 + 2\text{Re}\left[\mathcal{A}^{(1)*}_{\text{bkgd,0}}\mathcal{A}^{(1)}_{\text{bkgd,m}}\right]}_{\text{LO}} \\ &+ \underbrace{2\text{Re}\left[\mathcal{A}^{(1)*}_{\text{bkgd,0}}\mathcal{A}^{(2)}_{\text{bkgd,0}} + \mathcal{A}^{(1)*}_{\text{bkgd,m}}\mathcal{A}^{(2)}_{\text{bkgd,m}} + \mathcal{A}^{(1)*}_{\text{bkgd,0}}\mathcal{A}^{(2)}_{\text{bkgd,m}} + \mathcal{A}^{(2)*}_{\text{bkgd,0}}\mathcal{A}^{(1)}_{\text{bkgd,m}}\right]}_{\text{NLO (virtual)}} \\ &+ \ldots\end{aligned} \tag{5}$$

Similarly, for equation 4 this results in:

$$|\mathcal{A}_{\text{sgn}}|^2 = \underbrace{|\mathcal{A}^{(1)}_{\text{sgn}}|^2}_{\text{LO}} + \underbrace{2\text{Re}\left[\mathcal{A}^{(1)*}_{\text{sgn}}\mathcal{A}^{(2)}_{\text{sgn}}\right]}_{\text{NLO (virtual)}} + \ldots \tag{6}$$

And, finally, using equations 3 and 4, we can write the interference term as:

$$\begin{aligned}2\text{Re}\left[\mathcal{A}^{*}_{\text{sgn}}\mathcal{A}_{\text{bkgd}}\right] = &\underbrace{2\text{Re}\left[\mathcal{A}^{(1)*}_{\text{sgn}}\mathcal{A}^{(1)}_{\text{bkgd,0}} + \mathcal{A}^{(1)*}_{\text{sgn}}\mathcal{A}^{(1)}_{\text{bkgd,m}}\right]}_{\text{LO}} \\ &+ \underbrace{2\text{Re}\left[\mathcal{A}^{(1)*}_{\text{sgn}}\mathcal{A}^{(2)}_{\text{bkgd,0}} + \mathcal{A}^{(1)*}_{\text{sgn}}\mathcal{A}^{(2)}_{\text{bkgd,m}} + \mathcal{A}^{(2)*}_{\text{sgn}}\mathcal{A}^{(1)}_{\text{bkgd,0}} + \mathcal{A}^{(2)*}_{\text{sgn}}\mathcal{A}^{(1)}_{\text{bkgd,m}}\right]}_{\text{NLO (virtual)}} \\ &+ \ldots\end{aligned} \tag{7}$$

The sum of equations 5, 6, and 7 recovers the total transition amplitude in equation 1 up to LO, including two-loop virtual NLO corrections. For the full NLO QCD correction, one also needs to consider the real radiative contributions $gg\,(\to H+g) \to VV+g$ at one-loop. These can be split into the signal and the massive/massless background contributions along the lines described above.

The current status of the calculation of these amplitudes can be summarised as follows. The one-loop (LO) Higgs-mediated amplitude ($\mathcal{A}^{(1)}_{\text{sgn}}$) has been known for a long time, including full dependence on quark masses. The background amplitude, including both massive and massless contributions ($\mathcal{A}^{(1)}_{\text{bkgd,0}}+\mathcal{A}^{(1)}_{\text{bkgd,m}}$), has also been calculated at LO [11–13]. The LO computations for $gg\,(\to H) \to VV$ are available in the public codes `gg2VV` [14] and `MCFM` [15–17], and can also be obtained from standard one-loop generators such as `OpenLoops` [18].

The two-loop contributions to the Higgs-mediated amplitude ($\mathcal{A}^{(2)}_{\text{sgn}}$) are known [19–21], and the two-loop massless contributions to the background amplitude ($\mathcal{A}^{(2)}_{\text{bkgd,0}}$) were first computed in [22, 23]. However, the two-loop massive contributions to the background amplitude ($\mathcal{A}^{(2)}_{\text{bkgd,m}}$) were considerably more challenging to compute, due to the additional scale provided by the mass. This problem was previously circumvented by performing an expansion in $1/m_t$ in the heavy top limit [24–26]. The expansion in $1/m_t$ was only done for $gg \to ZZ$; for $gg \to WW$, only the massless contributions at NLO were considered.

The real corrections to the Higgs-mediated signal amplitude ($gg \to H+g \to VV+g$) have been known for many years [27], and the real corrections to the background amplitude ($gg \to VV+g$) can be obtained from automatic one-loop providers such as `OpenLoops` [18]. Additionally, one needs a means of combining the infrared divergences, arising separately in the virtual and the real corrections, to obtain a finite result. Since we consider NLO corrections, subtraction schemes for this purpose have been known for over two decades [28–30].

Thus, the only thing hindering the computation of the complete NLO predictions for off-shell Higgs production was the unknown two-loop massive background amplitude $\mathcal{A}^{(2)}_{\text{bkgd,m}}$. This situation changed recently with the calculation of the top quark contribution to the two-loop amplitude for on-shell Z pair production in gluon-gluon fusion ($gg \to ZZ$), while exact dependence on the top mass was retained [31, 32]. Similarly, the contribution of b and t loops to the two-loop amplitude for on-shell W pair production in gluon-gluon fusion ($gg \to WW$) was calculated, again retaining exact dependence on the top mass – the bottom quark was treated as massless [33]. We will use the amplitudes of references [31] and [33].

While the computation of these two-loop amplitudes is impressive from a technical point of view, it is extremely difficult to use them in practice. Indeed, for the case $gg \to ZZ$, the evaluation of the amplitude at a single phase space point takes approximately 3 hours on a single CPU core. For $gg \to WW$, this takes approximately 1 CPU hour – though in both cases, the speed strongly depends on fast read/write access to disk drives [31, 33]. At the time of writing, 1273 points have been evaluated for ZZ, with SM parameters $m_t = 173\,\text{GeV}$, $m_Z = 91\,\text{GeV}$, and renormalisation scale $\mu_\text{R} = m_Z$. For WW, 1156 points have been computed, with $m_t = 173\,\text{GeV}$, $m_W = 80\,\text{GeV}$, and renormalisation scale $\mu_\text{R} = 2m_W$.

In order to obtain cross sections, the relevant amplitude must be integrated over a phase space. This is normally done numerically using a Monte Carlo (MC) integration method, and studies at LO have shown that at least $\sim 10^4$ points are needed for reliable calculation of the cross section. The $\sim 10^3$ points that have currently been computed are therefore insufficient for a standard MC approach. Given the computational effort required to evaluate the $\mathcal{A}^{(2)}_{\text{bkgd,m}}$ amplitudes, we want to develop an interpolation strategy to perform this integration efficiently, by minimising the number phase-space points needed at which the amplitude is known exactly. This is especially useful if one wants to investigate how the cross sections respond to changes to SM parameters or renormalisation scales, requiring numerical re-evaluation of each point in the phase space, which demands significant computing time.

Although we want to employ the strategy to integrate the two-loop amplitudes, i.e. the terms in equations 5 and 7 containing $\mathcal{A}^{(2)}_{\text{bkgd,m}}$, here we will focus exclusively on the one-loop (LO) contributions, which occupy the same phase space. The reason for this is that the LO contributions are well-known[2] and relatively fast to evaluate numerically. This means that the integration of LO amplitudes can be performed using a more standard MC approach, which, as mentioned, is not suitable for directly integrating the two-loop amplitudes. We can then evaluate and benchmark the strategy that we develop against this standard approach. If we succeed in finding an efficient method that replicates the known results at LO using the same grid of few "exact" phase space points that we have available at NLO, we can have confidence that the method can be applied to NLO, too.

To facilitate interpolation of the $\mathcal{A}^{(2)}_{\text{bkgd,m}}$ amplitudes with only a limited number of points available, it is imperative that we construct the phase space wisely. That brings us to the next section, in which the chosen parametrisation of the phase space is presented.

[2] We take the amplitudes from OpenLoops [18].

III Parametrisation of the Lorentz-invariant phase space

In order to compute a total cross section for $gg\,(\rightarrow H) \rightarrow VV$, we must integrate the transition amplitudes over a phase space. This accounts for all the possible final state configurations, subject to the conservation of 4-momentum and on-shell condition of the VV final state. We perform this computation using Monte-Carlo integration through the `VEGAS` algorithm. `VEGAS` is based on importance sampling – this means that more points are sampled in regions of the phase space where the integrand is important. It constructs this probability distribution based on multiple passes over the integration region. Given the numerical difficulty in evaluating the integrand, as it contains the two-loop massive amplitudes, it is vital that we construct a parametrisation of the phase space (i.e. choose our integration variables) as effectively as possible. The chosen parametrisation is presented below.

The two incoming gluons have 4-momenta $\mathbf{P}_1$ and $\mathbf{P}_2$:

$$\mathbf{P}_1 = \frac{\sqrt{s}}{2}\,(x_1,\,0,\,0,\,x_1)\,,\quad \mathbf{P}_2 = \frac{\sqrt{s}}{2}\,(x_2,\,0,\,0,\,-x_2) \tag{8}$$

where $\sqrt{s}$ is the collider energy (13 TeV at the LHC), and x_i is the fraction of proton momentum carried by the ith incoming gluon. Denoting the parton distribution function (the probability that the ith gluon has a momentum fraction between x_i and $x_i + \mathrm{d}x_i$) with $f_i(x_i)\mathrm{d}x_i$, the differential cross section $\mathrm{d}\sigma$ can be written as

$$\mathrm{d}\sigma = \frac{1}{F}|\mathcal{A}|^2 f_1(x_1) f_2(x_2)\,\mathrm{d}x_1\,\mathrm{d}x_2\,\mathrm{d}\mathit{\Phi}. \tag{9}$$

Here $\mathcal{A}$ is the total transition amplitude, F accounts for the incoming particle flux, and $\mathrm{d}\mathit{\Phi}$ denotes the Lorentz-invariant phase space. We obtain the parton distribution function sets from `LHAPDF` [34].

For the case $gg \rightarrow VV$ with on-shell V, $\mathrm{d}\mathit{\Phi}$ takes the form

$$\mathrm{d}\mathit{\Phi} = \underbrace{(2\pi)^4\delta^4(\mathbf{P}_1 + \mathbf{P}_2 - \mathbf{P}_3 - \mathbf{P}_4)}_{\text{Conservation of 4-momentum}}\underbrace{\frac{\mathrm{d}^4 P_3}{(2\pi)^3 2E_3}\frac{\mathrm{d}^4 P_4}{(2\pi)^3 2E_4}}_{\text{Density of states}}\underbrace{\delta\big(\mathbf{P}_3\cdot\mathbf{P}_3 - m_V^2\big)\,\delta\big(\mathbf{P}_4\cdot\mathbf{P}_4 - m_V^2\big)}_{\text{On-shell condition}}, \tag{10}$$

where $\mathbf{P}_3 = (E_3,\,\mathbf{p}_3)$ and $\mathbf{P}_4 = (E_4,\,\mathbf{p}_4)$ are the 4-momenta of the VV final state, and m_V is the rest mass of V. The flux factor F is given by:

$$F = \frac{1}{4\,(\mathbf{P}_1\cdot\mathbf{P}_2)} = \frac{1}{2x_1 x_2 s}. \tag{11}$$

The 4-momenta $\mathbf{P}_3$ and $\mathbf{P}_4$ can be rewritten in terms of the transverse momentum $\mathbf{p}_\mathrm{T} := (p_x, p_y)$, transverse mass $m_\mathrm{T} := \sqrt{m_V^2 + p_\mathrm{T}^2}$, and rapidities $y := \frac{1}{2}\ln(E + p_z) - \frac{1}{2}\ln(E - p_z)$ of the final state particles:

$$\mathbf{P}_3 = (m_\mathrm{T}\cosh y_3,\,\mathbf{p}_\mathrm{T},\,m_\mathrm{T}\sinh y_3)\,,\quad \mathbf{P}_4 = (m_\mathrm{T}\cosh y_4,\,-\mathbf{p}_\mathrm{T},\,m_\mathrm{T}\sinh y_4)\,. \tag{12}$$

Performing this substitution of variables in equation 10, it becomes:

$$\mathrm{d}\mathit{\Phi} = \frac{\mathrm{d}^2 p_\mathrm{T}\,\mathrm{d}y_3\,\mathrm{d}y_4}{8\pi^2 s}\delta(x_1 - \overline{x}_1)\,\delta(x_2 - \overline{x}_2)\,, \tag{13}$$

with

$$\overline{x}_1 = \frac{m_\mathrm{T}}{\sqrt{s}}\,(\mathrm{e}^{y_3} + \mathrm{e}^{y_4})\,,\quad \overline{x}_2 = \frac{m_\mathrm{T}}{\sqrt{s}}\,\big(\mathrm{e}^{-y_3} + \mathrm{e}^{-y_4}\big)\,. \tag{14}$$

Then, using equations 11 and 13, we can write equation 9 as:

$$\mathrm{d}\sigma = \frac{1}{2\overline{x}_1\overline{x}_2 s}|\mathcal{A}|^2 f_1(\overline{x}_1) f_2(\overline{x}_2) \frac{\mathrm{d}^2 p_\mathrm{T}\,\mathrm{d}y_3\,\mathrm{d}y_4}{8\pi^2 s}. \tag{15}$$

Finally, we perform another change of variables to Δy, $\overline{y}$, and m_{VV}. The first two are the sum and difference of the rapidities of the final state particles respectively:

$$\Delta y := y_3 - y_4, \quad \overline{y} := \frac{y_3 + y_4}{2}. \tag{16}$$

The latter is the centre of mass energy of the VV final state:

$$m_{VV}^2 := (\mathbf{P}_3 + \mathbf{P}_4)^2 = 2m_\mathrm{T}^2(1 + \cosh\Delta y). \tag{17}$$

Completing this substitution of variables, equation 15 becomes:

$$\mathrm{d}\sigma = |\mathcal{A}|^2 f_1(\overline{x}_1) f_2(\overline{x}_2) \frac{\overline{x}_1\overline{x}_2}{32\pi(1 + \cosh\Delta y)\, m_{VV}^4}\,\mathrm{d}m_{VV}^2\,\mathrm{d}\Delta y\,\mathrm{d}\overline{y}\,\frac{\mathrm{d}\phi}{2\pi}, \tag{18}$$

where ϕ is the azimuthal angle around the z axis (such that $\mathrm{d}^2 p_\mathrm{T} = p_\mathrm{T}\,\mathrm{d}p_\mathrm{T}\,\mathrm{d}\phi$), and where

$$\begin{aligned} \overline{x}_1 &= \frac{2m_\mathrm{T}}{\sqrt{s}}\cosh\left(\frac{\Delta y}{2}\right)\mathrm{e}^{\overline{y}} = \frac{m_{VV}}{\sqrt{s}}\,\mathrm{e}^{\overline{y}} \\ \overline{x}_2 &= \frac{2m_\mathrm{T}}{\sqrt{s}}\cosh\left(\frac{\Delta y}{2}\right)\mathrm{e}^{-\overline{y}} = \frac{m_{VV}}{\sqrt{s}}\,\mathrm{e}^{-\overline{y}}. \end{aligned} \tag{19}$$

We choose to generate around fixed m_{VV}. For a given m_{VV}, the maximum value of Δy occurs when $m_\mathrm{T} = m_V$ (i.e. $\mathbf{p}_\mathrm{T} = \mathbf{0}$). This means:

$$m_{VV}^2 = 2m_V^2(1 + \cosh\Delta y_\mathrm{max}) \implies \Delta y_\mathrm{max} = \operatorname{arccosh}\left(\frac{m_{VV}^2}{2m_V^2} - 1\right). \tag{20}$$

It follows that the integration domains for m_{VV} and Δy are given by:

$$\begin{aligned} m_{VV}^2 &\in \left[4m_V^2,\ s\right] \\ \Delta y &\in [-\Delta y_\mathrm{max},\ \Delta y_\mathrm{max}]. \end{aligned} \tag{21}$$

The azimuthal angle is integrated over a full period:

$$\phi \in [0,\ 2\pi]. \tag{22}$$

For $\overline{y}$ we use the fact that the momentum of an incoming gluon cannot exceed that of the proton:

$$\begin{aligned} \overline{x}_1 \leq 1 &\implies \frac{m_{VV}}{\sqrt{s}}\mathrm{e}^{\overline{y}} \leq 1 \\ \overline{x}_2 \leq 1 &\implies \frac{m_{VV}}{\sqrt{s}}\mathrm{e}^{-\overline{y}} \leq 1, \end{aligned} \tag{23}$$

which tells us that

$$\overline{y} \in [-\overline{y}_\mathrm{max},\ \overline{y}_\mathrm{max}], \quad \overline{y}_\mathrm{max} = \frac{1}{2}\ln\left(\frac{1}{\tau}\right) \tag{24}$$

where

$$\tau := \overline{x}_1 \overline{x}_2 = \frac{m_{VV}^2}{s}. \tag{25}$$

Finally, using the fact that $\mathrm{d}\overline{x}_1 = \overline{x}_1 \mathrm{d}\overline{y}$, we can rewrite part of the integral as follows:

$$\int_{-\overline{y}_{\max}}^{\overline{y}_{\max}} f_1\left(\overline{x}_1\right) f_2\left(\overline{x}_2\right) \overline{x}_1 \overline{x}_2 \, \mathrm{d}\overline{y} = \tau \int_{\tau}^{1} f_1(\overline{x}_1) f_2\left(\frac{\tau}{\overline{x}_1}\right) \frac{\mathrm{d}\overline{x}_1}{\overline{x}_1}, \tag{26}$$

where the bounds of integration are justified by:

$$\begin{aligned} \overline{x}_1^{\max} &= \frac{m_{VV}}{\sqrt{s}} \mathrm{e}^{\overline{y}_{\max}} = 1 \\ \overline{x}_1^{\min} &= \frac{m_{VV}}{\sqrt{s}} \mathrm{e}^{-\overline{y}_{\max}} = \tau. \end{aligned} \tag{27}$$

So, after integrating out the azimuthal angle ϕ, the differential cross section can be written in the following form:

$$\boxed{\mathrm{d}\sigma = |\mathcal{A}|^2 \frac{1}{32\pi\left(1 + \cosh \Delta y\right) m_{VV}^4} \left[\tau \int_{\tau}^{1} f_1\left(\overline{x}_1\right) f_2\left(\frac{\tau}{\overline{x}_1}\right) \frac{\mathrm{d}\overline{x}_1}{\overline{x}_1}\right] \mathrm{d}m_{VV}^2 \, \mathrm{d}\Delta y,} \tag{28}$$

where the bounds of integration are given by equation 21. This form is useful because the term in the square brackets is returned by the public code `HOPPET` [35]. What remains is a two dimensional integral over m_{VV} and Δy.

Despite this efficient formulation of the phase space, $\sim 10^3$ phase space points are still not sufficient to reliably compute the integral, even if sampling grids are used. Therefore, we will formulate an interpolation strategy for the amplitudes – this is done in the next section.

IV Interpolation method for the top quark contribution to the two-loop amplitudes

The end goal is to be able to integrate components of the amplitudes containing $\mathcal{A}^{(2)}_{\mathrm{bkgd,m}}$ terms (see equations 5, 6, and 7) over the entire phase space. The difficulty is that the $\mathcal{A}^{(2)}_{\mathrm{bkgd,m}}$ components of the amplitude have only been computed at a limited set of points in the phase space, and, as described in section II, obtaining more points is computationally intensive. This motivates the development of an interpolation method for the $\mathcal{A}^{(2)}_{\mathrm{bkgd,m}}$ amplitudes, such that these integrals can be computed efficiently.

We begin with the aforementioned grid of 1273 points in the phase space at which the top quark contribution to the two-loop amplitude for $gg \to ZZ$ has already been computed [31]. The strategy is to populate this grid with the known exact LO amplitudes $\mathcal{A}^{(1)}_{\mathrm{bkgd,m}}$; since the LO amplitudes can be evaluated quickly, this allows us to compare how well the interpolation performs against a standard MC implementation.

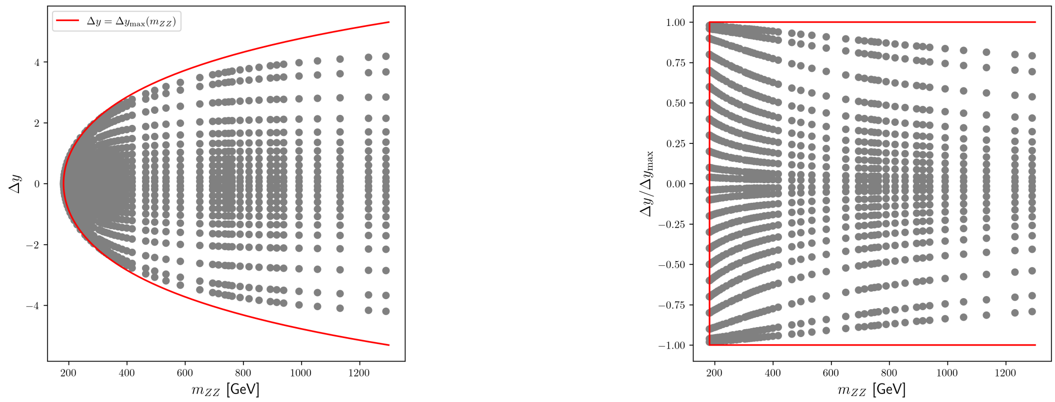

(a) **(b)**

Figure 3: Points in $(m_{ZZ}, \Delta y)$ at which the top quark contribution to the two-loop amplitude for $gg \to ZZ$ prompt production is known, in (a) the original and (b) the rectangular integration domain.

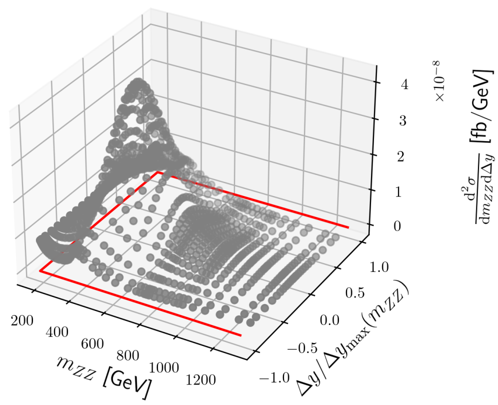

Figure 4: The grid from figure 3 populated with the LO total integration weights

The points are laid out in a grid of Mandelstam variables (s, t), which we can convert to a grid in $(m_{ZZ}, \Delta y)$ using:

$$m_{ZZ} = \sqrt{s}, \quad \Delta y = \ln\left[\frac{m_{ZZ}^2}{m_V^2 - t} - 1\right]. \tag{29}$$

The grid-points are shown in the two dimensional scatterplot in figure 3a, where the red line indicates the domain of integration. To facilitate our interpolation, it is convenient to map this domain to a rectangle. Doing so produces the scatterplot in figure 3b. Next, we populate the grid in $(m_{ZZ}, \Delta y/\Delta y_{\max})$ with the total integration weight at each point:

$$|\mathcal{A}^{(1)}_{\text{bkgd,m}}|^2 \frac{1}{32\pi\,(1+\cosh\Delta y)\, m_{VV}^4} \left[\tau \int_\tau^1 f_1\left(\overline{x}_1\right) f_2\left(\frac{\tau}{\overline{x}_1}\right) \frac{\mathrm{d}\overline{x}_1}{\overline{x}_1}\right]. \tag{30}$$

This results in the three dimensional scatterplot in figure 4.

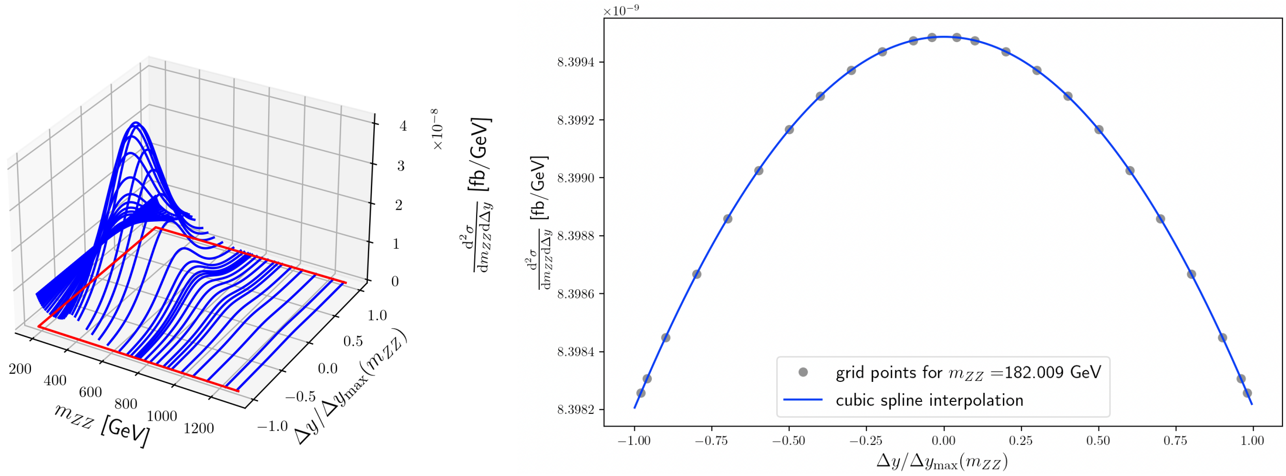

(a) (b)

Figure 5: One dimensional interpolation of lines in constant m_{ZZ}.

The grid is organised in lines of constant m_{ZZ}, allowing us to perform a one dimensional interpolation on each line – for this, the `CubicSpline` function from the `scipy.interpolate` library was used [36]. In brief, cubic splines are functions defined piecewise by third-order polynomials passing through a set of control points. The polynomials are fit between each two adjacent points such that the the first and second derivatives are continuous at the boundary, meaning the one dimensional interpolation is guaranteed to be smooth. The plot in figure 5a shows the interpolated lines in constant m_{ZZ}. Figure 5b shows an example of the one dimensional interpolation, performed for the line of grid-points with $m_{ZZ} = 182.009\,\text{GeV}$.

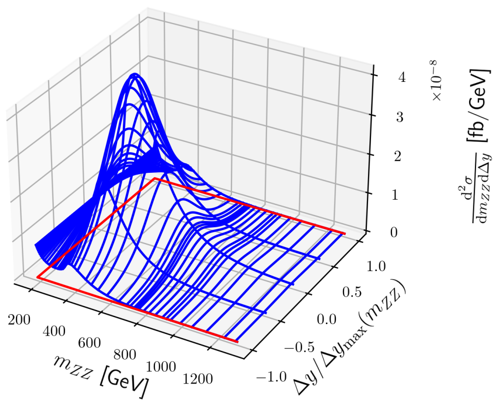

Figure 6: One dimensional interpolation of some lines in constant $\Delta y/\Delta y_{\max}$.

Next, we pick a line of constant $\Delta y/\Delta y_{\max}$. Along this line, we find the points of intersection with each of the lines in constant m_{ZZ}. These points can then also be interpolated using cubic splines. Figure 6 shows interpolated lines at five values of constant $\Delta y/\Delta y_{\max}$. For added clarity, figure 7 shows a two dimensional projection of the interpolation lines, in both the original integration domain (7a) and the rectangular integration domain (7b). We are slowly building a 'web' of one dimensional interpolated lines. Note that the intersections of the lines do not necessarily correspond to one of the 1273 phase space points at which the amplitude is known.

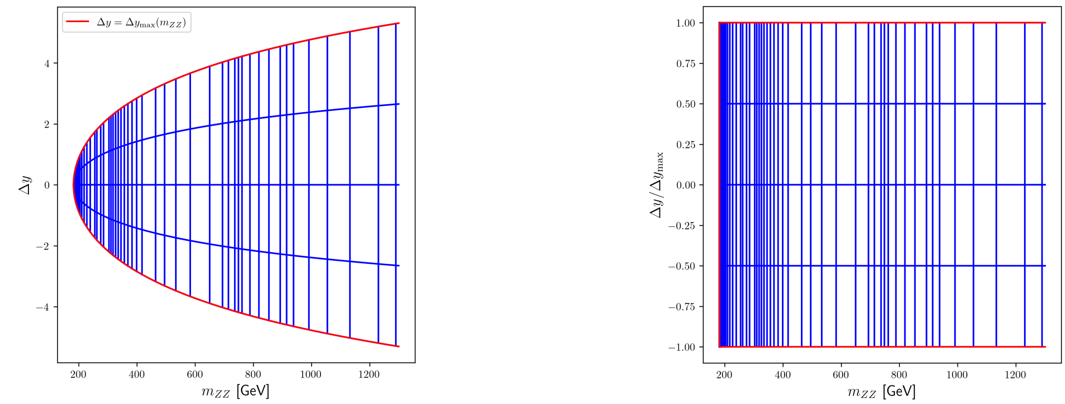

(a) **(b)**

Figure 7: Two dimensional projections of the interpolated lines in figure 6, shown in both (a) the original and (b) the rectangular integration domain.

This procedure can be repeated until a smooth surface can be constructed. For the $\mathcal{A}^{(1)}_{\text{bkgd,m}}$ amplitudes used in our example, this results in the surfaces shown in figure 8. We can directly integrate over this surface to obtain a cross section.

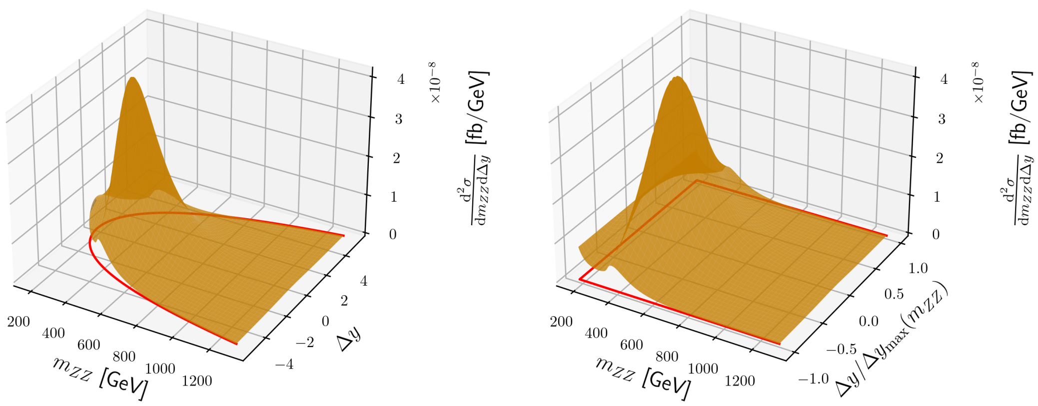

(a) **(b)**

Figure 8: Smooth interpolated surface of the total integration weight at each point in the phase space, for the LO top quark contributions to the $gg \to ZZ$ background amplitude. Shown in both (a) the original and (b) the rectangular integration domain.

The method was tested for two more scenarios, whose integrands show very different behaviour in the phase space. Specifically, the interference between b and t and the interference between $udsc$ and bt for $gg \to ZZ$ prompt production. In other words, we consider equation 30 with the replacements:

$$|\mathcal{A}^{(1)}_{\text{bkgd,m}}|^2 \to \text{Re}\left[\mathcal{A}^{(1)}_{\text{bkgd},t}\mathcal{A}^{(1)*}_{\text{bkgd},b}\right] \text{ and } |\mathcal{A}^{(1)}_{\text{bkgd,m}}|^2 \to \text{Re}\left[\mathcal{A}^{(1)}_{\text{bkgd},bt}\mathcal{A}^{(1)*}_{\text{bkgd},udsc}\right]. \tag{31}$$

The surfaces obtained from interpolating the integrands in each case are shown in figures 9 and 10 respectively. This illustrates that our interpolation method works for a range of different behaviours.

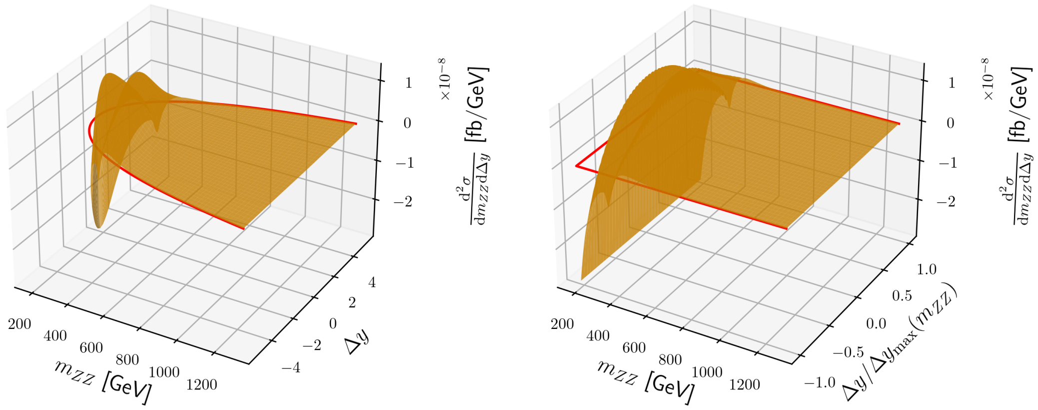

(a) **(b)**

Figure 9: Smooth interpolated surface of the total integration weight at each point in the phase space, for the LO contribution from interference between b and t to the $gg \to ZZ$ background amplitude. Shown in both (a) the original and (b) the rectangular integration domain.

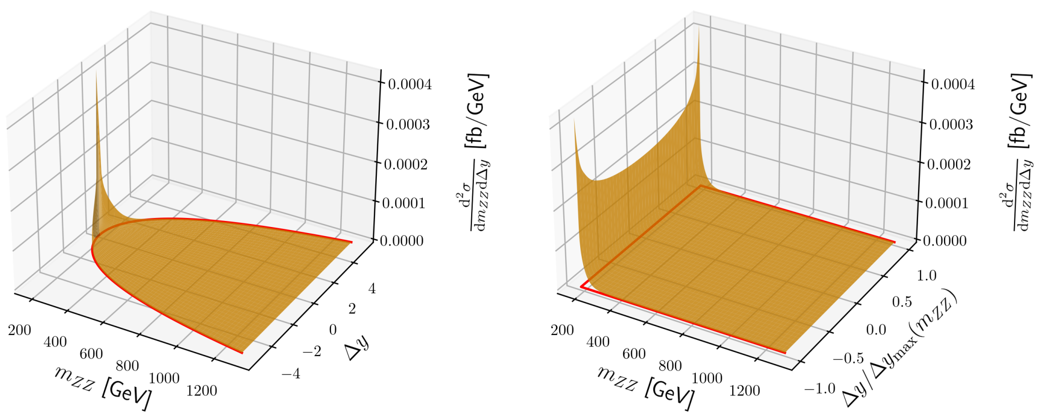

(a) **(b)**

Figure 10: Smooth interpolated surface of the total integration weight at each point in the phase space, for the LO contribution from interference between $udsc$ and bt to the $gg \to ZZ$ background amplitude. Shown in both (a) the original and (b) the rectangular integration domain.

V Results and discussion

We now report results for various contributions to the LO cross sections for $gg \to ZZ$ production at the $\sqrt{s} = 13\,\text{TeV}$ LHC, obtained using a standard MC implementation and using the interpolation method discussed in the previous section.

We employ the following parameters in our computation:

$$\begin{aligned} m_t &= 173\,\text{GeV}, & G_F &= 1.16639 \times 10^{-5}\,\text{GeV}^{-2}, \\ m_Z &= 91\,\text{GeV}, & g_w^2 &= 4\sqrt{2} m_W^2 G_F, \\ m_W &= 80\,\text{GeV}, & \cos\theta_W &= m_W/m_Z. \end{aligned} \tag{32}$$

The masses of Z, W, and t are set to integers, in line with [31], and we use NNPDF3.1 [37] parton distribution functions to obtain the LO results. The renormalisation and factorisation scales are set at a dynamical value $\mu_\text{R} = \mu_\text{F} = m_{VV}/2$. No phase space cuts are made. We use $\alpha_\text{s}(m_Z) = 0.118$ for the strong coupling constant.

Integration over the one-loop (LO) massive contributions only ($\mathcal{A}^{(1)}_{\text{bkgd,m}}$) using the interpolation method yields:

$$\sigma^{\text{LO, interpolated}}_{\text{bkgd, top only}}(gg \to ZZ) = (4.12540 \pm 0.00047) \times 10^{-2}\,\text{fb}, \tag{33}$$

which is $\sim 0.04\%$ off the result obtained using a standard MC implementation:

$$\sigma^{\text{LO}}_{\text{bkgd, top only}}(gg \to ZZ) = (4.127586 \pm 0.000083) \times 10^{-2}\,\text{fb}. \tag{34}$$

The agreement is very close – numerical control at this level is perfectly sufficient for phenomenological studies at the LHC. Note that the uncertainties are numerical errors resulting from the integration.

For the case of b and t interference at LO (Re $\left[\mathcal{A}^{(1)}_{\text{bkgd},t}\mathcal{A}^{(1)*}_{\text{bkgd},b}\right]$), agreement is within $\sim 0.3\%$:

$$\begin{aligned} \sigma^{\text{LO, interpolated}}_{\text{bkgd, } b \text{ and } t \text{ interf.}}(gg \to ZZ) &= (8.6909 \pm 0.0029) \times 10^{-3}\,\text{fb}, \\ \sigma^{\text{LO}}_{\text{bkgd, } b \text{ and } t \text{ interf.}}(gg \to ZZ) &= (8.66391 \pm 0.00030) \times 10^{-3}\,\text{fb}. \end{aligned} \tag{35}$$

The agreement with the standard MC result, while still sufficient, is slightly less good. This can be explained as follows. Cubic splines are well-suited for interpolation, but not ideal for extrapolation – the polynomial used to interpolate the last two adjacent grid-points is extended to the edge of the phase space. This means that if the regions near the edge of the phase space are not very important to the integral, the interpolation will work extremely well. This is the case for the top quark contributions only, as clearly the peak region in figure 8 is well away from boundary of the integration domain. For the case of b and t interference, there is a steep region at low invariant mass – see figure 9. The extrapolation that occurs in this region towards the edges of the phase space contributes significantly to the integral. This leads to a slightly larger deviation of the cross section from the value obtained by standard MC integration. A straightforward way to overcome this would be to simply remove the need to extrapolate – this can be done by constructing a grid that goes right to the edges of the phase space. This would require to the order of ~ 100 additional points to be computed, which is feasible.

For the same reasons described above, in the case of $udsc$ and bt interference at LO (Re $\left[\mathcal{A}^{(1)}_{\text{bkgd},udsc}\mathcal{A}^{(1)*}_{\text{bkgd},bt}\right]$)

the interpolated amplitude is $\sim 3\%$ off the result obtained from a standard MC implementation:

$$\begin{aligned}
&\sigma^{\text{LO, interpolated}}_{\text{bkgd, } udsc \text{ and } tb \text{ interf.}}(gg \to ZZ) = 0.9235 \pm 0.0011\,\text{fb},\\
&\sigma^{\text{LO}}_{\text{bkgd, } udsc \text{ and } tb \text{ interf.}}(gg \to ZZ) = 0.949804 \pm 0.000024\,\text{fb}.
\end{aligned} \tag{36}$$

Here the main contributions to the integral are concentrated in regions of low invariant mass, with almost asymptotic behaviour – see figure 10. Again, any extrapolation in this extremely steep region leads to (occasionally large) deviations from the exact result. This can be solved by, as mentioned, computing additional points near the boundary of the phase space. However, for quite extreme behaviour such as this, it could also be beneficial to construct a different parametrisation to distribute the contributions to the integral more evenly over the phase space – this is left for future work. Cubic splines have the potential to behave erratically when faced with asymptotic behaviour such as in this example. In general, it is best to proceed with caution, and use the three dimensional plots to maintain control of the behaviour of the interpolation.

VI Conclusions

In this report we presented an interpolation method that can be used to integrate the two-loop massive amplitudes of $gg \to VV$ prompt production – this is the last remaining hurdle towards the calculation of the full NLO corrections to $gg\,(\to H) \to VV$. We tested the method at LO, where amplitudes can be evaluated efficiently, so that the results can be compared to those obtained through a standard MC implementation. We observe agreement at the level of a few per mille for integrands with reasonable behaviour in the phase space. Numerical control at this level is more than satisfactory. Indeed, other sources of uncertainty, e.g. the scale uncertainty, are at the level of 10% at NLO and will dominate the theoretical uncertainties [24]. We pointed out that the agreement could be improved further by computing additional points near boundaries of the phase space, which would remove the need to extrapolate. For cases where the integrand exhibits more extreme behaviour, if these are encountered, a reparametrisation of the phase space should be considered – a task that is left for future work.

The next step is to apply this interpolation method to calculate the full NLO corrections to $gg\,(\to H) \to VV$, and to include final states with leptonic decays. Given the promising performance of the interpolation method at one-loop, and the fact that it can be directly applied at two-loop, there is now a direct path to computing the full NLO corrections to off-shell Higgs production at the LHC.

References

[1] Georges Aad et al. "Observation of a new particle in the search for the Standard Model Higgs boson with the ATLAS detector at the LHC". In: *Phys. Lett. B* 716 (2012), pp. 1–29. DOI: 10.1016/j.physletb.2012.08.020. arXiv: 1207.7214 [hep-ex].

[2] Serguei Chatrchyan et al. "Observation of a New Boson at a Mass of 125 GeV with the CMS Experiment at the LHC". In: *Phys. Lett. B* 716 (2012), pp. 30–61. DOI: 10.1016/j.physletb.2012.08.021. arXiv: 1207.7235 [hep-ex].

[3] Nikolas Kauer and Giampiero Passarino. "Inadequacy of zero-width approximation for a light Higgs boson signal". In: *JHEP* 08 (2012), p. 116. DOI: 10.1007/JHEP08(2012)116. arXiv: 1206.4803 [hep-ph].

[4] Fabrizio Caola and Kirill Melnikov. "Constraining the Higgs boson width with ZZ production at the LHC". In: *Phys. Rev. D* 88 (2013), p. 054024. DOI: 10.1103/PhysRevD.88.054024. arXiv: 1307.4935 [hep-ph].

[5] G. Aad et al. "Constraints on the off-shell Higgs boson signal strength in the high-mass ZZ and WW final states with the ATLAS detector". In: *The European Physical Journal C* 75.7 (2015). ISSN: 1434-6052. DOI: 10.1140/epjc/s10052-015-3542-2. URL: http://dx.doi.org/10.1140/epjc/s10052-015-3542-2.

[6] V. Khachatryan et al. "Search for Higgs boson off-shell production in proton-proton collisions at 7 and 8 TeV and derivation of constraints on its total decay width". In: *Journal of High Energy Physics* 2016.9 (2016). ISSN: 1029-8479. DOI: 10.1007/jhep09(2016)051. URL: http://dx.doi.org/10.1007/JHEP09(2016)051.

[7] A.M. Sirunyan et al. "Measurements of the Higgs boson width and anomalous HVV couplings from on-shell and off-shell production in the four-lepton final state". In: *Physical Review D* 99.11 (2019). ISSN: 2470-0029. DOI: 10.1103/physrevd.99.112003. URL: http://dx.doi.org/10.1103/PhysRevD.99.112003.

[8] V. Khachatryan et al. "Limits on the Higgs boson lifetime and width from its decay to four charged leptons". In: *Physical Review D* 92.7 (2015). ISSN: 1550-2368. DOI: 10.1103/physrevd.92.072010. URL: http://dx.doi.org/10.1103/PhysRevD.92.072010.

[9] V. Khachatryan et al. "Constraints on the Higgs boson width from off-shell production and decay to Z-boson pairs". In: *Physics Letters B* 736 (2014), pp. 64–85. ISSN: 0370-2693. DOI: 10.1016/j.physletb.2014.06.077. URL: http://dx.doi.org/10.1016/j.physletb.2014.06.077.

[10] M. Aaboud et al. "Constraints on off-shell Higgs boson production and the Higgs boson total width in ZZ→4 and ZZ→22 final states with the ATLAS detector". In: *Physics Letters B* 786 (2018), pp. 223–244. ISSN: 0370-2693. DOI: 10.1016/j.physletb.2018.09.048. URL: http://dx.doi.org/10.1016/j.physletb.2018.09.048.

[11] E. W. Nigel Glover and J. J. van der Bij. "Z boson pair production via gluon fusion". In: *Nucl. Phys. B* 321 (1989), pp. 561–590. DOI: 10.1016/0550-3213(89)90262-9.

[12] T. Matsuura and J. J. van der Bij. "Characteristics of leptonic signals forZ boson pairs at hadron colliders". In: *Zeitschrift für Physik C Particles and Fields* 51.2 (1991), pp. 259–265. DOI: 10.1007/BF01475793. URL: https://doi.org/10.1007/BF01475793.

[13] C. Zecher, T. Matsuura, and J. J. van der Bij. "Leptonic signals from off-shell Z boson pairs at hadron colliders". In: *Z. Phys. C* 64 (1994), pp. 219–226. DOI: 10.1007/BF01557393. arXiv: hep-ph/9404295.

[14] T. Binoth, N. Kauer, and P. Mertsch. "Gluon-induced QCD corrections to pp —> ZZ —> l anti-l l-prime anti-l-prime". In: *16th International Workshop on Deep Inelastic Scattering and Related Subjects*. July 2008, p. 142. DOI: 10.3360/dis.2008.142. arXiv: 0807.0024 [hep-ph].

[15] John M. Campbell, R. Keith Ellis, and Ciaran Williams. "Bounding the Higgs Width at the LHC Using Full Analytic Results for $gg- > e^-e^+\mu^-\mu^+$". In: *JHEP* 04 (2014), p. 060. DOI: 10.1007/JHEP04(2014)060. arXiv: 1311.3589 [hep-ph].

[16] John M. Campbell, R. Keith Ellis, and Ciaran Williams. "Vector boson pair production at the LHC". In: *JHEP* 07 (2011), p. 018. DOI: 10.1007/JHEP07(2011)018. arXiv: 1105.0020 [hep-ph].

[17] John M. Campbell, R. Keith Ellis, and Ciaran Williams. "Bounding the Higgs width at the LHC: Complementary results fromH→WW". In: *Physical Review D* 89.5 (2014). ISSN: 1550-2368. DOI: 10.1103/physrevd.89.053011. URL: http://dx.doi.org/10.1103/PhysRevD.89.053011.

[18] Fabio Cascioli, Philipp Maierhofer, and Stefano Pozzorini. "Scattering Amplitudes with Open Loops". In: *Phys. Rev. Lett.* 108 (2012), p. 111601. DOI: 10.1103/PhysRevLett.108.111601. arXiv: 1111.5206 [hep-ph].

[19] U. Aglietti et al. "Analytic Results for Virtual QCD Corrections to Higgs Production and Decay". In: *JHEP* 01 (2007), p. 021. DOI: 10.1088/1126-6708/2007/01/021. arXiv: hep-ph/0611266.

[20] M. Spira et al. "Higgs boson production at the LHC". In: *Nuclear Physics B* 453.1-2 (1995), pp. 17–82. ISSN: 0550-3213. DOI: 10.1016/0550-3213(95)00379-7. URL: http://dx.doi.org/10.1016/0550-3213(95)00379-7.

[21] Robert V Harlander and Philipp Kant. "Higgs production and decay: analytic results at next-to-leading order QCD". In: *Journal of High Energy Physics* 2005.12 (2005), pp. 015–015. ISSN: 1029-8479. DOI: 10.1088/1126-6708/2005/12/015. URL: http://dx.doi.org/10.1088/1126-6708/2005/12/015.

[22] Fabrizio Caola et al. "Two-loop helicity amplitudes for the production of two off-shell electroweak bosons in gluon fusion". In: *JHEP* 06 (2015), p. 129. DOI: 10.1007/JHEP06(2015)129. arXiv: 1503.08759 [hep-ph].

[23] Andreas von Manteuffel and Lorenzo Tancredi. "The two-loop helicity amplitudes for $gg \to V_1V_2 \to$ 4 leptons". In: *JHEP* 06 (2015), p. 197. DOI: 10.1007/JHEP06(2015)197. arXiv: 1503.08835 [hep-ph].

[24] Fabrizio Caola et al. "QCD corrections to vector boson pair production in gluon fusion including interference effects with off-shell Higgs at the LHC". In: *JHEP* 07 (2016), p. 087. DOI: 10.1007/JHEP07(2016)087. arXiv: 1605.04610 [hep-ph].

[25] Kirill Melnikov and Matthew Dowling. "Production of two Z-bosons in gluon fusion in the heavy top quark approximation". In: *Physics Letters B* 744 (2015), pp. 43–47. ISSN: 0370-2693. DOI: 10.1016/j.physletb.2015.03.030. URL: http://dx.doi.org/10.1016/j.physletb.2015.03.030.

[26] John M. Campbell et al. "Two loop correction to interference in gg → ZZ". In: *Journal of High Energy Physics* 2016.8 (2016). ISSN: 1029-8479. DOI: 10.1007/jhep08(2016)011. URL: http://dx.doi.org/10.1007/JHEP08(2016)011.

[27] R.K. Ellis et al. "Higgs decay to +−A possible signature of intermediate mass Higgs bosons at high energy hadron colliders". In: *Nuclear Physics B* 297.2 (1988), pp. 221–243. ISSN: 0550-3213. DOI: https://doi.org/10.1016/0550-3213(88)90019-3. URL: https://www.sciencedirect.com/science/article/pii/0550321388900193.

[28] S. Catani and M.H. Seymour. "The dipole formalism for the calculation of QCD jet cross sections at next-to-leading order". In: *Physics Letters B* 378.1-4 (1996), pp. 287–301. ISSN: 0370-2693. DOI: 10.1016/0370-2693(96)00425-x. URL: http://dx.doi.org/10.1016/0370-2693(96)00425-X.

[29] S. Catani and M.H. Seymour. "A general algorithm for calculating jet cross sections in NLO QCD". In: *Nuclear Physics B* 485.1-2 (1997), pp. 291–419. ISSN: 0550-3213. DOI: 10.1016/s0550-3213(96)00589-5. URL: http://dx.doi.org/10.1016/S0550-3213(96)00589-5.

[30] S. Frixione, Z. Kunszt, and A. Signer. "Three-jet cross sections to next-to-leading order". In: *Nuclear Physics B* 467.3 (1996), pp. 399–442. ISSN: 0550-3213. DOI: 10.1016/0550-3213(96)00110-1. URL: http://dx.doi.org/10.1016/0550-3213(96)00110-1.

[31] Christian Brønnum-Hansen and Chen-Yu Wang. "Top quark contribution to two-loop helicity amplitudes for Z boson pair production in gluon fusion". In: *JHEP* 05 (2021), p. 244. DOI: 10.1007/JHEP05(2021)244. arXiv: 2101.12095 [hep-ph].

[32] Bakul Agarwal, Stephen P. Jones, and Andreas von Manteuffel. "Two-loop helicity amplitudes for gg → ZZ with full top-quark mass effects". In: *Journal of High Energy Physics* 2021.5 (2021). ISSN: 1029-8479. DOI: 10.1007/jhep05(2021)256. URL: http://dx.doi.org/10.1007/JHEP05(2021)256.

[33] Christian Brønnum-Hansen and Chen-Yu Wang. "Contribution of third generation quarks to two-loop helicity amplitudes for W boson pair production in gluon fusion". In: *JHEP* 01 (2021), p. 170. DOI: 10.1007/JHEP01(2021)170. arXiv: 2009.03742 [hep-ph].

[34] Andy Buckley et al. "LHAPDF6: parton density access in the LHC precision era". In: *The European Physical Journal C* 75.3 (2015). ISSN: 1434-6052. DOI: 10.1140/epjc/s10052-015-3318-8. URL: http://dx.doi.org/10.1140/epjc/s10052-015-3318-8.

[35] Gavin P. Salam and Juan Rojo. "A Higher Order Perturbative Parton Evolution Toolkit (HOPPET)". In: *Comput. Phys. Commun.* 180 (2009), pp. 120–156. DOI: 10.1016/j.cpc.2008.08.010. arXiv: 0804.3755 [hep-ph].

[36] Pauli Virtanen et al. "SciPy 1.0: Fundamental Algorithms for Scientific Computing in Python". In: *Nature Methods* 17 (2020), pp. 261–272. DOI: 10.1038/s41592-019-0686-2.

[37] Richard D. Ball et al. "Parton distributions for the LHC Run II". In: *JHEP* 04 (2015), p. 040. DOI: 10.1007/JHEP04(2015)040. arXiv: 1410.8849 [hep-ph].